Electronic Supplementary Material (ESI) for Nanoscale.

Supporting Information

Simultaneous Reversible Tuning of H^+ and Zn^{2+} Coinsertion in MnO_2 Cathode for High-Capacity Aqueous Zn-Ion Battery

Zhoutai Shang,[a,b,1] Hong Zhang,[a,b,1] Mingli Wang,[a] Qianwang Chen[a,b] and Ke Lu[a,b,*]

[a]Institutes of Physical Science and Information Technology, Key Laboratory of Structure and Functional Regulation of Hybrid Materials of Ministry of Education, Anhui Graphene Engineering Laboratory, Anhui University, Hefei, Anhui 230601, China. E-mail: luke@ahu.edu.cn (K.L.)

[b]Hefei National Laboratory for Physical Sciences at the Microscale, University of Science and Technology of China, Hefei, Anhui 230026, China.

[1]Z.S. and H.Z. contributed equally to this work.

Experimental

Materials synthesis

Preparation of MnO_2 nanofiber. The α-manganese dioxide was synthesized by hydrothermal method. 2.0289 g $MnSO_4 \cdot H_2O$ (Adamas) and 8 ml 0.5 M H_2SO_4 (Adamas) were dissolved in 300 ml deionized water and stir at room temperature, then 1.264g of $KMnO_4$ (Adamas) were dissolved in 90 ml deionized water and slowly added to the solution. Stir the mixture at room temperature for 2 h. The solution was then transferred to a Teflon-lined autoclave and heated at 120 °C for 12 h, α-MnO_2 nanofiber were obtained. After autoclave cooling to room temperature, The solution was filtered and cleaned, and then vacuum-dried for 12 h.

Preparation of MnO_2@MnHCF-PPy cathodes. 0.3 g of α-MnO_2 nanofibers was dispersed in a mixture of 20 mL ethanol and 20 ml deionized water. 0.4 g $K_4Fe(CN)_6$ (Adamas) added in a mixture of 20 mL ethanol, 20 mL deionized water , 2 ml 0.5 M HCl (Adamas) and 100 μl pyrrole (Adamas). Slowly added to the solution and stir the mixture at ice-water bath for 2 h, the resulting solution is rinsed with plenty of deionized water and dried, corresponding sample was marked as MnO_2@MnHCF-PPy. MnO_2@PPy cathode was prepared through the same procedure without the addition of $K_4Fe(CN)_6$.

Materials characterization

Representative X-ray diffraction (XRD) patterns were acquired using a Bruker D2 Phaser X-ray diffractometer (Cu Kα, radiation, Germany) over the wide 2θ range of 10°-80°. X-ray photoelectron spectroscopy (XPS) measurements were performed on Thermal Escalab 250 X-ray photoelectron spectrometer. The morphology of the sample was analyzed by Hitachi SU8010 FESEM or JEOL JEM-2100F FETEM and EDS at 200 kV accelerating voltage.

Electrochemical measurements

The modified or unmodified α-MnO_2 nanofibers, multi-walled carbon nanotube and polyvinylidene fluoride in a weight ratio of 7:2:1 in N-methyl pyrrolidone solvent. Formed a uniform mix of slurry, evenly coated to the hydrophilic carbon paper ang The α-MnO_2 mass loading is 1.0-2.0 mg cm^{-2}. Zn/MnO_2 batteries were assembled using an α-MnO_2 electrode as the cathode, glass fibre as the separator and Zn slice as the anode in CR2025 coin cells under ambient conditions. 2M $ZnSO_4$ aqueous solution was used as the electrolyte. The batteries charge/discharge was carried out on Neware CT-4008 analyzers between 1.0 and 1.9 V at different current densities. Cyclic voltammograms (CV) were measured using a Germy electrochemical workstation. The preparation conditions of $ZnSO_4$/poly(vinyl alcohol) ($ZnSO_4$-PVA) gel electrolyte are as follows: 3g $ZnSO_4$ was dissolved in 30ml deionized water, then 3g PVA (PVA-117, $M_w \sim 145\,000$) was added to mix thoroughly and heated at 85°C with intense agitation for 4h. To prepare a solid-state flexible Zn-ion batteries, the cathode and anode are immersed in a gel electrolyte and then cured under environmental conditions to remove excess moisture.

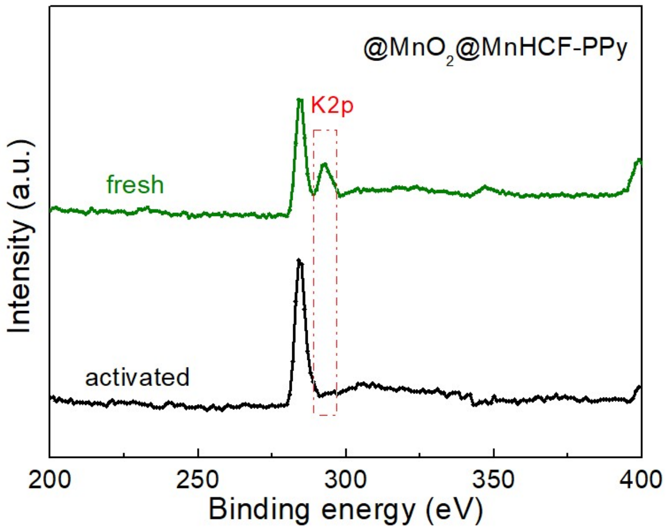

Figure S1: XPS survey spectra of the MnO$_2$@MnHCF-PPy sample before and after activation process.

After pre-activation (0.1C, 3 cycle), the potassium ions were extracted from MnKCF during the first few cycles and did not interrupt the subsequent reversible intercalation/deintercalation of zinc ions.

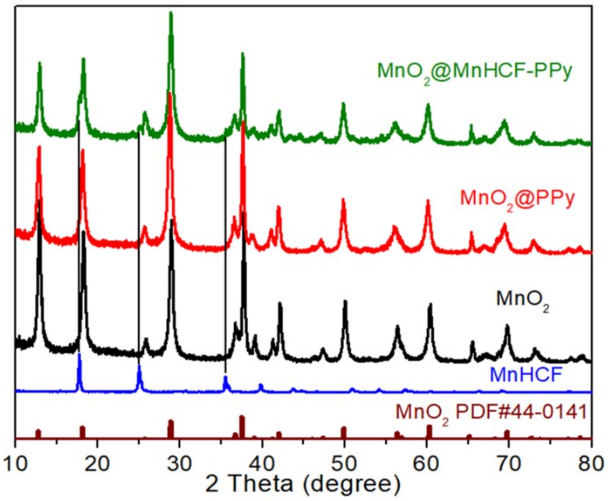

Figure S2: XRD patterns of bare MnO$_2$, modified MnO$_2$ and pure MnHCF powder.

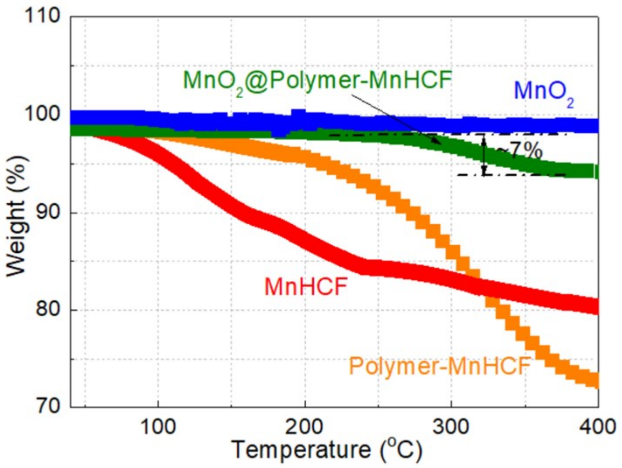

Figure S3: TGA curve of different materials.

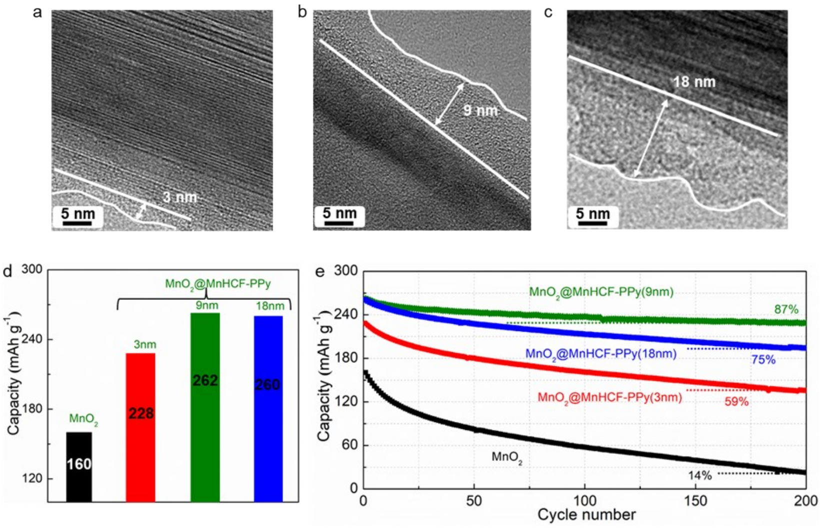

Figure S4: TEM images of MnO_2@MnHCF-PPy composites with varied MnHCF-PPy thickness (a: 3nm; b: 9nm; c: 18nm), (d) initial discharge capacities and (e) cycling stability of different MnO_2 samples.

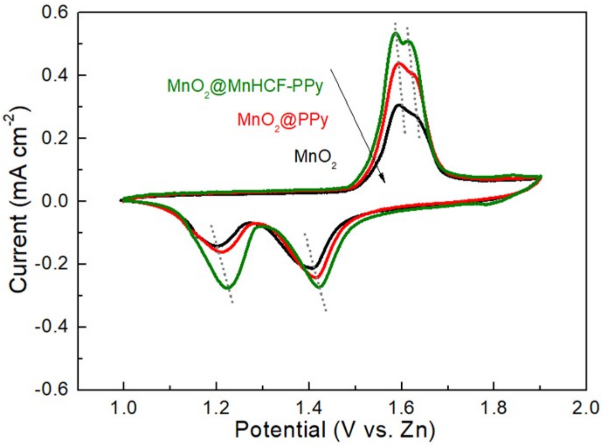

Figure S5: CV curves of the MnO_2, MnO_2@PPy and MnO_2@MnHCF-PPy electrodes in 2 M $ZnSO_4$ electrolyte at 0.1 mV s^{-1}.

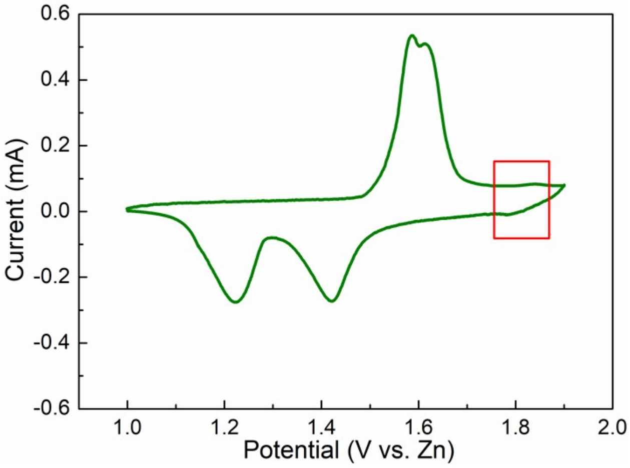

Figure S6: CV curve of MnO_2@MnHCF-PPy cathode at 0.1 mV s^{-1}.

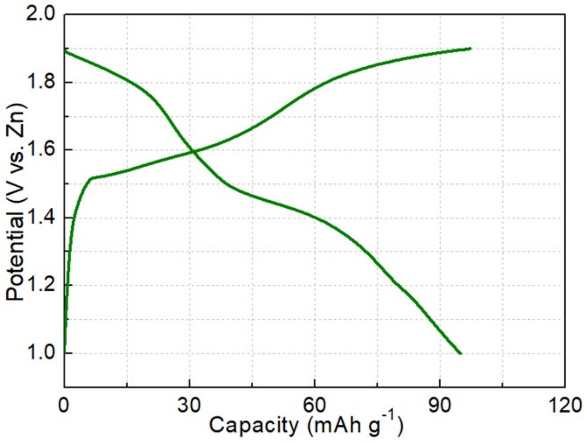

Figure S7: Galvanostatic charge-discharge profiles of MnHCF at 0.5C.

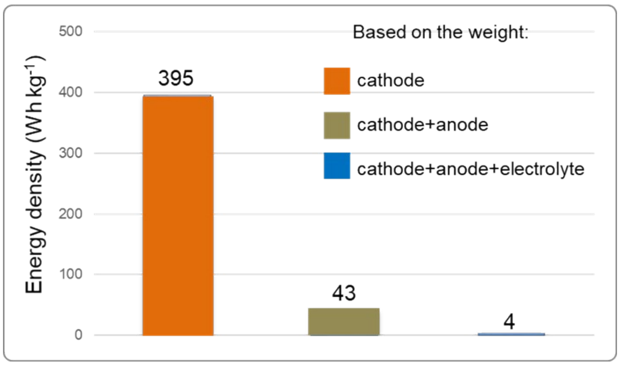

Figure S8: The calculated energy densities of Zn-MnO_2 full batteries, where the influence of the weight of cathode, anode and electrolyte on the calculation was considered.

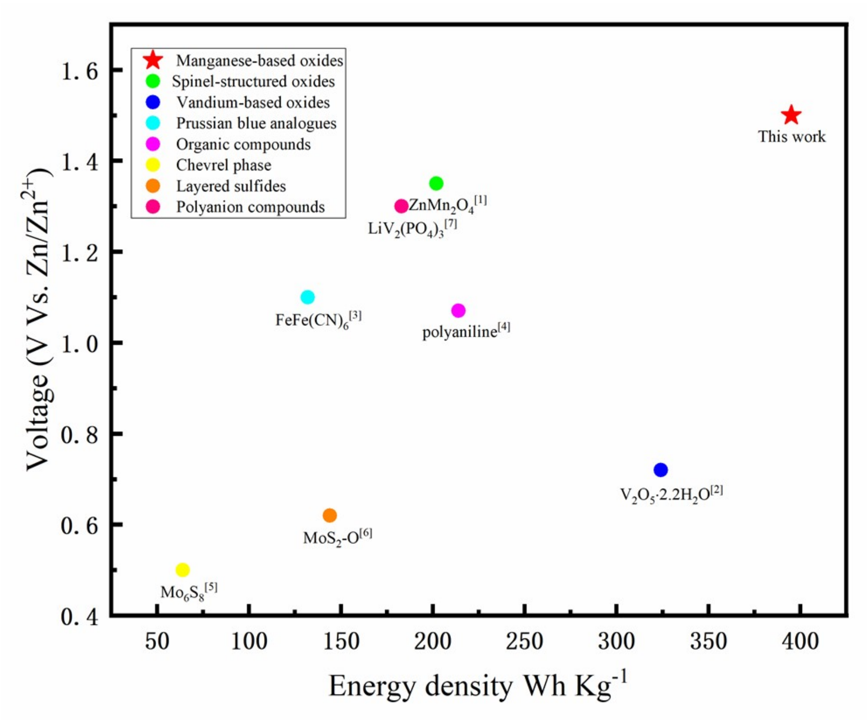

Figure S9: The comparison of representative cathodes in ZIBs.

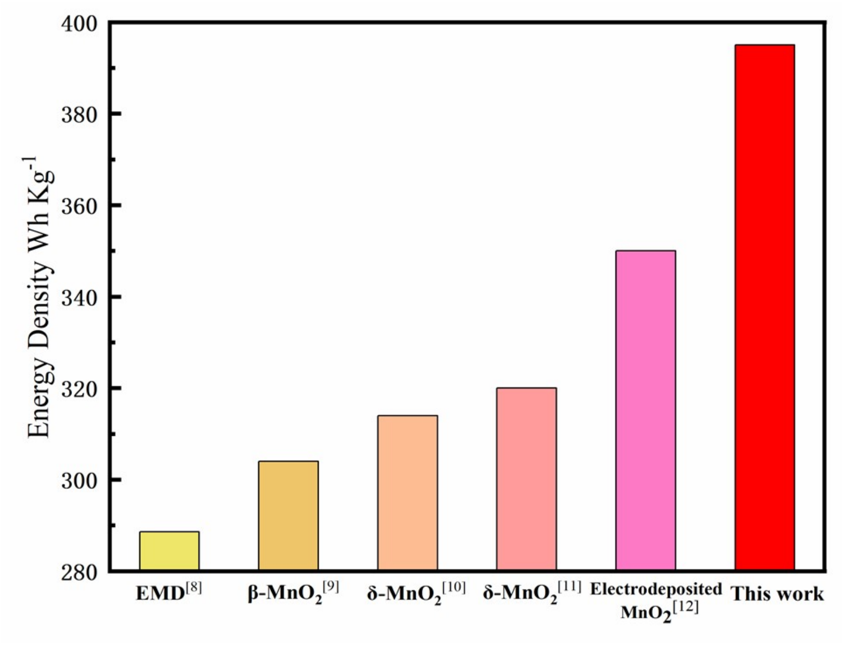

Figure S10: The comparison for energy densities of representative cathodes in ZIBs.

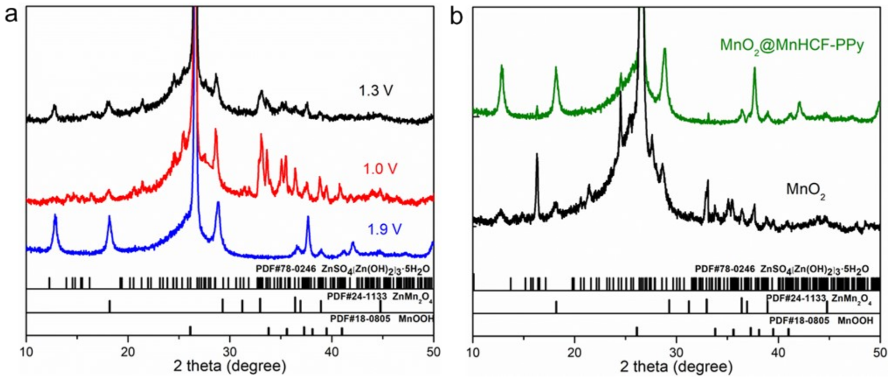

Figure S11: (a) *Ex-situ* XRD patterns of the MnO_2@MnHCF-PPy cathode at different states; (b) Comparison of XRD patterns of different cycled MnO_2 cathodes.

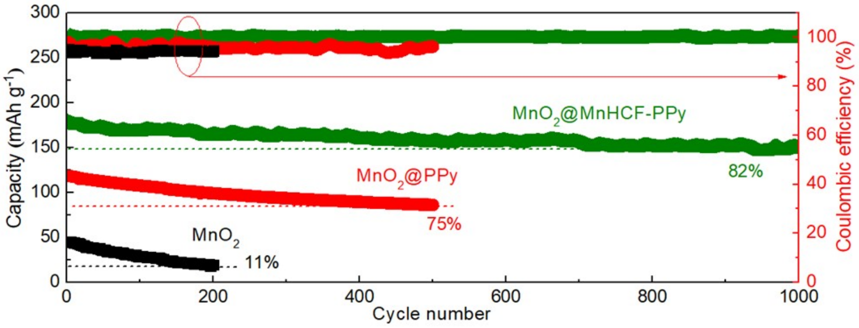

Figure S12: Cycling performance and the corresponding Coulombic efficiency tested at 5C.

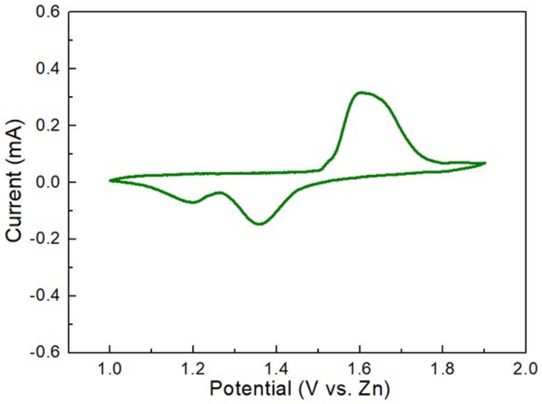

Figure S13: CV (0.1 mV s^{-1}) profile of the flexible MnO_2-Zn cell.

Table S1: Comparison of cycling performance of various cathodes for aqueous zinc ion battery.

Cathode	Capacity (current density)	Cycling performance (current density)	*Ref.*
MnO_2@MnHCF-PPy	**263 mAh g^{-1} (at 0.15A g^{-1})**	**87%/200 cycles (0.3 A g^{-1})**	**This work**
V_2O_5	470 mAh g^{-1} (at 0.2A g^{-1})	91.1%/4000 cycles (5 A g^{-1})	*ACS Energy Lett.* 2018, 3, 1366.
$V_5O_{12}\cdot 6H_2O$	354.8 mAh g^{-1} (at 0.5A g^{-1})	97.4%/100 cycles (0.5 A g^{-1})	*Adv. Funct. Mater.* 2019, 1807331.
PANI-intercalated MnO_2	280 mAh g^{-1} (at 0.2A g^{-1})	90%/200 cycles (0.2 A g^{-1})	*Nat. Commun.* 2018, 9, 2906.
δ -MnO_2	243 mAh g^{-1} (at 0.1A g^{-1})	89.5%/500 cycles (0.5 A g^{-1})	*Chem. Sci., 2021, 12, 5843*
WS_2-200	179.99 mAh g^{-1} (at 0.2A g^{-1})	25%/20 cycles (0.2 A g^{-1})	*J. Alloys Compd.* 2022, 894, 162391.
α-MnO_2/rGO-PPy	248.8 mAh g^{-1} (at 0.5A g^{-1})	85.9%/100 cycles (0.5 A g^{-1})	*J. Mater. Sci.* 2021, 56, 16582.
VO_2(B)@CFS	386.2 mAh g^{-1} (at 0.2A g^{-1})	88.6%/100 cycles (0.2 A g^{-1})	*CrystEngComm* 2021, 23, 8650.
MoS_2@CNTs	180.0 mAh g^{-1} (at 0.1A g^{-1})	80.1%/500 cycles (1 A g^{-1})	*ChemElectroChem* 2020, 7, 4218.
V_2O_5/rGO	175 mAh g^{-1} (at 0.1A g^{-1})	77.3%/200 cycles (0.1 A g^{-1})	*Ionics* 2020, 26, 5607.

Supplementary References

[1] N. Zhang, F. Cheng, Y. Liu, Q. Zhao, K. Lei, C. Chen, J. Chen, *J. Am. Chem. Soc.* **2016**, *138*, 12894-12901.

[2] J. Zhao, H. Ren, Q. Liang, D. Yuan, S. Xi, C. Wu, Q. Yan, *Nano Energy* **2019**, *62*, 94-102.

[3] Z. Liu, G. Pulletikurthi, F. Endres, *ACS Appl. Mater. Interfaces* **2016**, *8*, 12158-12164.

[4] F. Wan, L. Zhang, X. Wang, S. Bi, Z. Niu, J. Chen, *Adv. Funct. Mater.* **2018**, *28*, 1804975.

[5] M. S. Chae, J. W. Heo, S. C. Lim, S. T. Hong, *Inorg. Chem.* **2016**, *55*, 3294-3301.

[6] H. Liang, Z. Cao, F. Ming, W. Zhang, D. H. Anjum, Y. Cui, H. N. Alshareef, *Nano Lett.* **2019**, *19*, 3199-3206.

[7] F. Wang, E. Hu, W. Sun, T. Gao, X. Ji, X. Fan, C. Wang, *Energy Environ. Sci.* **2018**, *11*, 3168-3175.

[8] H. Yang, Z. Chang, Y. Qiao, H. Deng, X. Mu, P. He, H. Zhou, *Angew. Chem., Int. Ed.* **2020**, *59*, 9377-9381.

[9] N. Zhang, F. Cheng, J. Liu, L. Wang, X. Long, X. Liu, J. Chen, *Nat. Commun.* **2017**, *8*, 1-9.

[10] M. H. Alfaruqi, S. Islam, D. Y. Putro, V. Mathew, S. Kim, J. Jo, J. Kim, *Electrochim. Acta* **2018**, *276*, 1-11.

[11] M. H. Alfaruqi, J. Gim, S. Kim, J. Song, D. T. Pham, J. Jo, J. Kim, *Electrochem. Commun.* **2015**, *60*, 121-125.

[12] G. Sun, X. Jin, H. Yang, J. Gao, L. Qu, *J. Mater. Chem. A* **2018**, *6*, 10926-10931.